p53 mutants cooperate with HIF-1 in transcriptional regulation of extracellular matrix components to promote tumor progression

Ivano Amelio[a,1,2], Mara Mancini[b,1], Varvara Petrova[a], Rob A. Cairns[c], Polina Vikhreva[a], Sara Nicolai[a], Alberto Marini[a], Alexey A. Antonov[a], John Le Quesne[a,d], Juvenal D. Baena Acevedo[e], Kate Dudek[a], Gabriella Sozzi[f], Ugo Pastorino[g], Richard A. Knight[a], Tak W. Mak[c], and Gerry Melino[a,h,2]

[a]Medical Research Council (MRC) Toxicology Unit, University of Cambridge, LE1 9HN Leicester, United Kingdom; [b]Biochemistry Laboratory, Istituto Dermopatico dell'Immacolata, Istituto di Ricovero e Cura a Carattere Scientifico (IDI-IRCCS), 00167 Rome, Italy; [c]The Campbell Family Institute for Breast Cancer Research at Princess Margaret Cancer Centre, University Health Network, Toronto, ON, Canada M5G 2C1; [d]Department of Cancer Studies, University of Leicester, LE1 9HN Leicester, United Kingdom; [e]Department of Genetics, University of Leicester, LE1 9HN Leicester, United Kingdom; [f]Tumour Genomics, Fondazione Istituto Di Ricovero e Cura a Carattere Scientifico, Istituto Nazionale Tumori, 20133 Milan, Italy; [g]Thoracic Surgery, Fondazione Istituto Di Ricovero e Cura a Carattere Scientifico, Istituto Nazionale Tumori, 20133 Milan, Italy; and [h]Department of Experimental Medicine and Surgery, IDI-IRCCS, University of Rome Tor Vergata, 00133 Rome, Italy

Mutations in the *TP53* gene and microenvironmentally driven activation of hypoxia-inducible factor-1 (HIF-1) typically occur in later stages of tumorigenesis. An ongoing challenge is the identification of molecular determinants of advanced cancer pathogenesis to design alternative last-line therapeutic options. Here, we report that p53 mutants influence the tumor microenvironment by cooperating with HIF-1 to promote cancer progression. We demonstrate that in non-small cell lung cancer (NSCLC), p53 mutants exert a gain-of-function (GOF) effect on HIF-1, thus regulating a selective gene expression signature involved in protumorigenic functions. Hypoxia-mediated activation of HIF-1 leads to the formation of a p53 mutant/HIF-1 complex that physically binds the SWI/SNF chromatin remodeling complex, promoting expression of a selective subset of hypoxia-responsive genes. Depletion of p53 mutants impairs the HIF-mediated up-regulation of extracellular matrix (ECM) components, including type VIIa1 collagen and laminin-γ2, thus affecting tumorigenic potential of NSCLC cells in vitro and in mouse models in vivo. Analysis of surgically resected human NSCLC revealed that expression of this ECM gene signature was highly correlated with hypoxic tumors exclusively in patients carrying p53 mutations and was associated with poor prognosis. Our data reveal a GOF effect of p53 mutants in hypoxic tumors and suggest synergistic activities of p53 and HIF-1. These findings have important implications for cancer progression and might provide innovative last-line treatment options for advanced NSCLC.

p53 | HIF | microenvironment | chromatin architecture | SWI/SNF

The *TP53* gene (encoding the corresponding tumor suppressor protein p53) is the most frequently mutated gene in all human cancers. These sequence alterations typically occur as missense mutations that abolish its tumor-suppressive activity and lead to new oncogenic forms of p53 (1–5). The gain-of-function (GOF) properties of mutant p53 have partially been explained by its ability to physically interact with other transcriptional factors and deregulate their transcriptional abilities (6–9). Indeed, although canonical p53-mediated tumor suppression is strictly related to cell cycle arrest/apoptosis, accumulating evidence highlights the involvement of mutant forms of p53 in processes such as cancer metabolism, invasion/metastasis, and tumor microenvironment interactions (10, 11). However, understanding of the impact of p53 mutants in different cellular, mutational, and microenvironmental backgrounds is limited; despite this, it would be critical to dissect the basis of the oncogenic phenotype associated with mutant p53 and consequentially accelerate improvement of the management of oncological patients.

At the stage at which mutations in the *TP53* gene occur, cancer cells have frequently already been exposed to reduced oxygen

tension, which further promotes cancer progression through the activation of hypoxia-inducible factor-1 (HIF-1) (12–16). Adaptation to the drop in oxygen level is indeed a key determinant for progression of cancer toward the more advanced stages (12, 15). The hypoxic microenvironment causes cancer cells to co-opt HIF-dependent processes, which provides all of the required features for cancer progression. HIF-1 coordinates the transcriptional program required to acquire proangiogenic, invasive, and metastatic properties, as well as metabolic adaptations and stemness, which, collectively, constitute the lethal cancer phenotype (17).

Here, we report that GOF p53 mutants co-opt HIF-1 in hypoxic non-small cell lung cancer (NSCLC) cells, thus inducing a selective HIF-1–dependent transcriptional response that promotes a non–cell-autonomous protumorigenic signaling. A molecular complex, including mutant p53 and HIF-1, directly promotes transcriptional expression of extracellular matrix (ECM) components,

Significance

Expression in cancer cells of novel proteins generated by mutations in the *TP53* gene is an important prognostic factor; however, how p53 mutants promote cancer progression is largely unknown. Here, we describe a molecular mechanism of gain-of-function by mutant p53 in hypoxic non-small cell lung cancer (NSCLC) cells. We identified the existence of a hypoxia-inducible factor-1 (HIF-1)/mutant p53 complex, exerting transcriptional control of a specific subset of protumorigenic genes, codifying for extracellular matrix (ECM) components. Employing in vivo cancer models and analyzing clinical material, we demonstrate that these ECM components substantially contribute to the synergistic protumorigenic activity of p53 mutants and HIF-1. Our data indicate that HIF-1/mutant p53 cross-talk is an innovative potential therapeutic target to treat advanced NSCLC.

CELL BIOLOGY

including type VIIa1 collagen and laminin-γ2. Mechanistically, recruitment of the SWI/SNF chromatin remodeling complex determines selectivity of p53 mutants on this specific subset of hypoxia-responsive genes. Modulation of the HIF-1/p53 mutant/ECM axis influences the tumorigenic phenotype of NSCLC cells in vitro and in mouse models in vivo. Clinical evidence indicates that this ECM gene signature was highly correlated with hypoxic tumors exclusively in patients carrying p53 mutations and was associated with poor prognosis. Our findings suggest potential alternative avenues for last-line treatment options for advanced NSCLC harboring mutant p53.

Results

Hypoxia-Induced HIF-1 Binds p53 Mutant and Drives It on the Chromatin. Mutations of the *TP53* gene commonly occur with intratumor hypoxia in later stages of tumor progression. Since the life expectancy of patients with concurrent mutations at the *TP53* locus and activation of hypoxic signaling is substantially lower than predicted from the simple additive effect of these two prognostic factors considered individually (Fig. 1*A*), we investigate here the specific molecular pathways responsible for the synergism between p53 mutants and hypoxia. Subcellular fractionation revealed that hypoxia (1% O_2) promoted enrichment of mutant p53 protein content in the chromatin fraction of two different NSCLC cell lines, NCI-H1155 (expressing p53 R273H) and NCI-H23 (expressing p53 R246I) (Fig. 1 *B* and *C*). No effect of hypoxia on the p53 protein level was observed in whole-cell extracts (*SI Appendix*, Fig. S1 *A* and *B*). This result indicates that hypoxia does not alter the expression level of the p53 R273H and p53 R246I proteins. Because HIF-1 plays a predominant role in the response to low oxygen concentrations, we examined whether HIF-1 has a direct role in driving the binding of mutant p53 to chromatin. Silencing HIF-1α dramatically abolished the accumulation of p53 mutants in the chromatin-bound fractions of cells treated with 1% O_2 (Fig. 1*D*). Additionally, overexpression of constitutively stable hydroxylated mutant HIF-1α [HA–HIF-1α PA: P402A/P464A (18)] also increased the binding of mutant p53 to the chromatin of cells grown in normoxia (Fig. 1*E*). Consistently, cobalt chloride ($CoCl_2$), which selectively stabilizes HIF-1α, recapitulated the effect of hypoxia on the interaction of p53 mutants with chromatin (*SI Appendix*, Fig. S1 *D* and *E*), which was rescued by HIF-1α depletion (*SI Appendix*, Fig. S2 *A* and *C*). As a comparison, we tested whether wild-type (wt) p53 adopted similar behavior at low oxygen concentrations. In the wt p53-expressing NSCLC cell line A549, hypoxia did not alter the binding of wt p53 to chromatin (*SI Appendix*, Fig. S2*B*), HIF-1α depletion consistently lacked an effect on the wt p53 content in the chromatin-bound fraction (*SI Appendix*, Fig. S2*C*). In contrast to p53 mutants, wt p53 showed up-regulated total protein levels in experiments of hypoxia and $CoCl_2$ treatment (*SI Appendix*, Fig. S1*C*). In addition, wt p53 physically bound HIF-1α through its DNA-binding domain (DBD) (*SI Appendix*, Fig. S2*D*), although HIF-1α appeared to be unstable within the molecular complex with full-length p53. Indeed, consistent with the previously reported negative regulation of wt p53 on HIF-1α stability, depletion of wt p53 increased normoxic levels of HIF-1α (*SI Appendix*, Fig. S2*E*). These last results were in agreement with previous studies, reporting the hypoxia-dependent stabilization of wt p53 (19, 20), a negative regulation of HIF-1α stability following physical binding to wt p53 (21–23), and an involvement of this interplay in p53-mediated hypoxic cell death (24–26).

HIF-1/p53 Mutant Complex Regulates Transcription of ECM Genes. We next investigated the molecular basis underlying the binding of mutant p53 to the chromatin under hypoxic stress. Coimmunoprecipitation experiments revealed a physical interaction between HIF-1α and the endogenous mutants p53 R273H and p53 R246I in NSCLC cell lines cultured in the presence of $CoCl_2$ (Fig. 1*F* and *SI Appendix*, Fig. S3*A*). Similarly, a proximity ligation assay (PLA)

confirmed the presence of a nuclear molecular complex, including mutant p53 and HIF-1α, under hypoxic conditions or upon HIF-1α stabilization by $CoCl_2$ treatment (*SI Appendix*, Fig. S3 *B* and *C*). We next mapped the interaction between HIF-1α and p53 mutant. We generated different constructs expressing Myc- or Flag-tagged domains of HIF-1α or p53 R273H, respectively (*SI Appendix*, Fig. S3 *D* and *E*). We then overexpressed these fragments in the p53$^{-/-}$ NSCLC cell line NCI-H1299, together with full-length HA-p53 R273H or Myc–HIF-1α, respectively. Coimmunoprecipitation clearly revealed that the N-terminal fragment of HIF-1α (HIF-1α$^{1–330}$) and the DBD of p53 R273H were involved in the physical interaction (Fig. 1 *G* and *H*). HIF-1α$^{1–330}$ contains the DBD [basic helix–loop–helix (bHLH) domain] and the Per–Arnt–Sim (PAS)-A/B domain, which interact with HIF-1β, the oxygen-insensitive subunit of HIF-1 (13). In addition, considering the presence of the bHLH and PAS-A/B domains at the HIF-1β N terminus, we explored whether HIF-1β interacts with p53 mutants to form a preexisting complex that is potentially present under normoxic conditions. However, a PLA showed no preexisting binding between HIF-1β and mutant p53 under normoxia but did reveal significant accumulation of the HIF-1β/mutant p53 complex when HIF-1α was stabilized via $CoCl_2$ treatment (*SI Appendix*, Fig. S3*F*). This requirement of the HIF-1α subunit for the binding of HIF-1β to mutant p53 indicated the existence of a complex consisting of mutant p53 and fully transcriptionally active HIF-1 (the HIF-1α/HIF-1β complex) under hypoxic conditions.

Missense mutations in p53 inactivate its DNA-binding ability, but recent data suggest that interactions with active transcription factors can mediate a p53 mutant-dependent transcriptional effect, which underlies its GOF properties (1, 9, 27). Therefore, we explored whether interaction with HIF-1 and accumulation on the chromatin under hypoxic stress could lead to the production of a specific mutant p53/hypoxia-dependent gene expression signature. We depleted p53 R273H from NCI-H1155 cells using siRNA, followed by an 8-h incubation in 1% O_2. Up-regulation of well-established hypoxic genes (*SI Appendix*, Fig. S4*A*), as well as accumulation of the hypoxia-dependent L-enantiomer of hydroxyglutarate (28, 29), confirmed successful activation of the hypoxia response in our cellular model (*SI Appendix*, Fig. S6 *B* and *C*). Then, we performed a global gene expression analysis (*SI Appendix*, Fig. S4 *B–F*). Comparison of the gene expression signatures associated with p53 R273H deficiency under normoxic and hypoxic conditions revealed a subgroup of ∼300 genes that are regulated by mutant p53 predominantly during hypoxic stress (Fig. 2*A*). Mutant p53 deficiency did not alter the entire HIF-1–dependent signature (*SI Appendix*, Fig. S5 *A* and *B*), indicating the selective regulation of certain hypoxia-responsive genes by mutant p53. In addition, there was no overlap with the wt p53-dependent gene expression signature in hypoxic conditions (*SI Appendix*, Fig. S2 *F* and *G*). To define the functional categories of this subgroup of 300 p53 mutant/hypoxia-dependent genes, we performed pathway analysis (Fig. 2*B*). The most highly represented pathway was "cellular movement," which was clearly associated with the propensity of cancer cells to disseminate into metastatic foci. This property was also represented in other categories, such as "cell morphology" and "cell interaction," and this observation suggests the ability of this mutant p53/hypoxia-dependent gene expression signature to influence the interaction of the tumor with the external microenvironment. Several genes encoding components of the ECM, such as collagens and laminin subunits, were included in a "cellular movement" group. The ECM is dynamically modulated, particularly in a hypoxic microenvironment, by multiple cell types, including cancer cells, thus promoting cancer progression. Indeed, changes in the composition and overall content of the ECM influence both its biophysical and biological properties, and these functions of the ECM, in turn, significantly affect tumor and stromal cell properties, such as proliferation and motility [reviewed by Gilkes et al. (17)]. Therefore, we
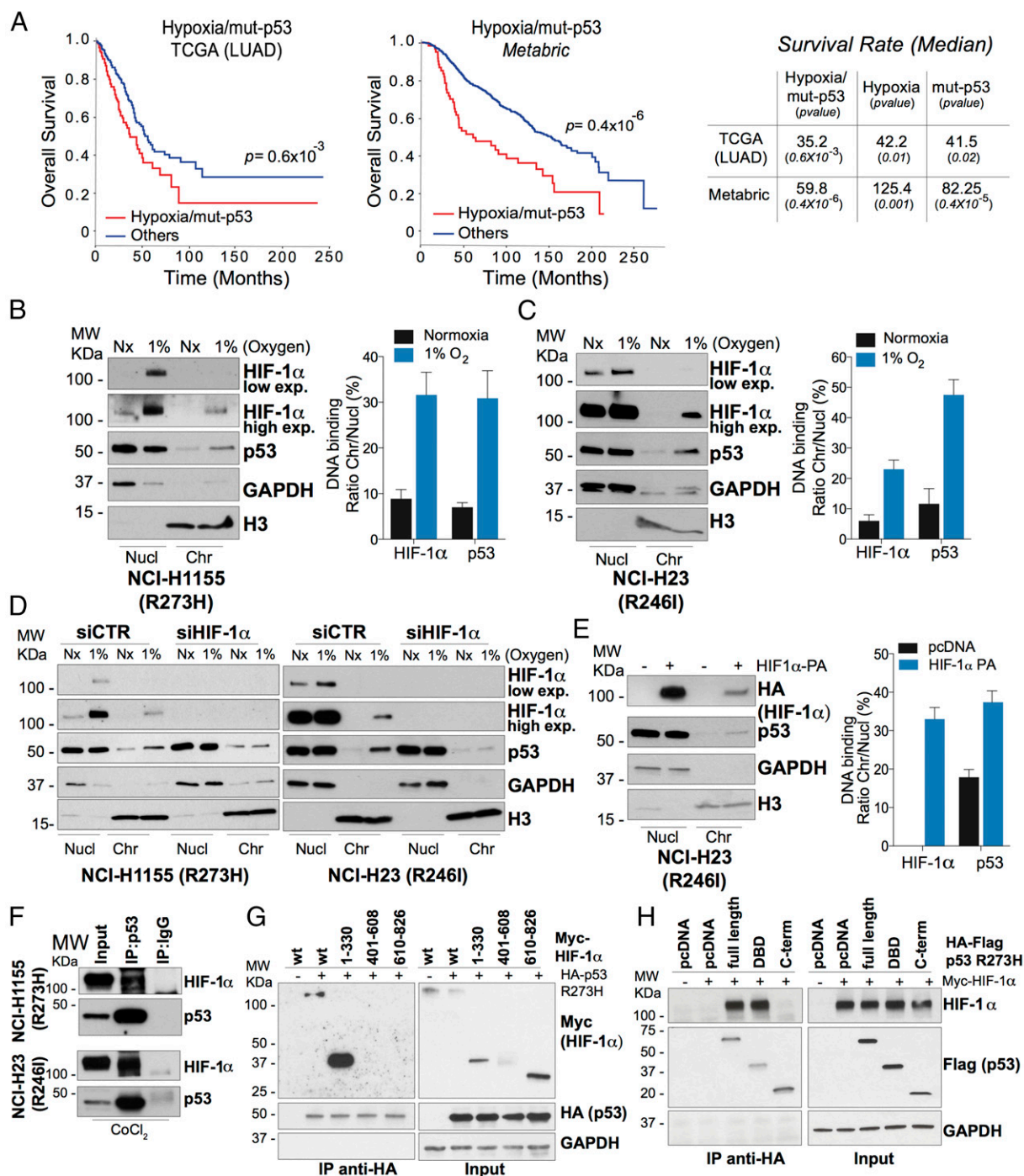
Fig. 1. Hypoxia-driven HIF-1 promotes the binding of p53 mutants to genomic DNA. (*A*) Kaplan–Meier plot indicating the overall survival estimates for patients with NSCLC presenting a mutation in the TP53 gene and activation of hypoxia (measured as a signature, including 10 different hypoxia-responsive genes). Datasets: The Cancer Genome Atlas (TCGA) lung adenocarcinoma (LUAD) and METABRIC breast cancer. The *P* value is indicated in the panel. "Others" indicates all of the samples not included in the hypoxia/mut-p53 groups (samples not presenting concurrent high signature and p53 mutant status). The table displays the median survival (months) of the patients comprising the different subgroups. (*B* and *C*) Western blot analysis of subcellular fractions (nuclear-soluble and chromatin-bound fractions) of NCI-H1155 and NCI-H23 cells treated with 1% oxygen for 4 h. Histograms show the ratio of Chr-bound/Nucl protein contents calculated via densitometry of Western blots. Chr, chromatin-bound fraction; Nucl, soluble nuclear fraction; MW, molecular weight (molecular mass); Nx, normoxia. (*D*) Western blot analysis of subcellular fractions of NCI-H1155 and NCI-H23 cells treated with 1% oxygen for 4 h following HIF-1α depletion using siRNA. CTR, control. (*E*) Western blot analysis of nuclear-soluble and chromatin-bound fractions of NCI-H23 cells overexpressing the HA-tagged HIF-1α PA mutant. The histogram shows the ratio of chromatin-bound/nuclear protein contents calculated via densitometry of Western blots. Error bars (in *B*, *C*, and *E*) indicate the SD of three densitometry measurements. (*F*) Coimmunoprecipitation of endogenous HIF-1α with p53 mutants (p53 R273H from NCI-H1155 cells and p53 R246I from NCI-H23 cells) in cells treated with 250 μM CoCl$_2$ for 4 h. IP, immunoprecipitation. (*G*) Coimmunoprecipitation assay of NCI-H1299 cells treated with 800 μM CoCl$_2$ and expressing HA-p53 R273H and different HIF-1α fragments, including the Myc-tagged N-terminal region HIF-1α, the Myc-tagged central domain HIF-1α$^{401–608}$, and the C-terminal region HIF-1α$^{610–826}$. (*H*) Coimmunoprecipitation assay of NCI-H1299 cells treated with 800 μM CoCl$_2$ and expressing Myc-HIF-1α and different fragments of HA-Flag–tagged p53 R273H DBD and HA-Flag–tagged p53 C-terminal (C-term) domain.
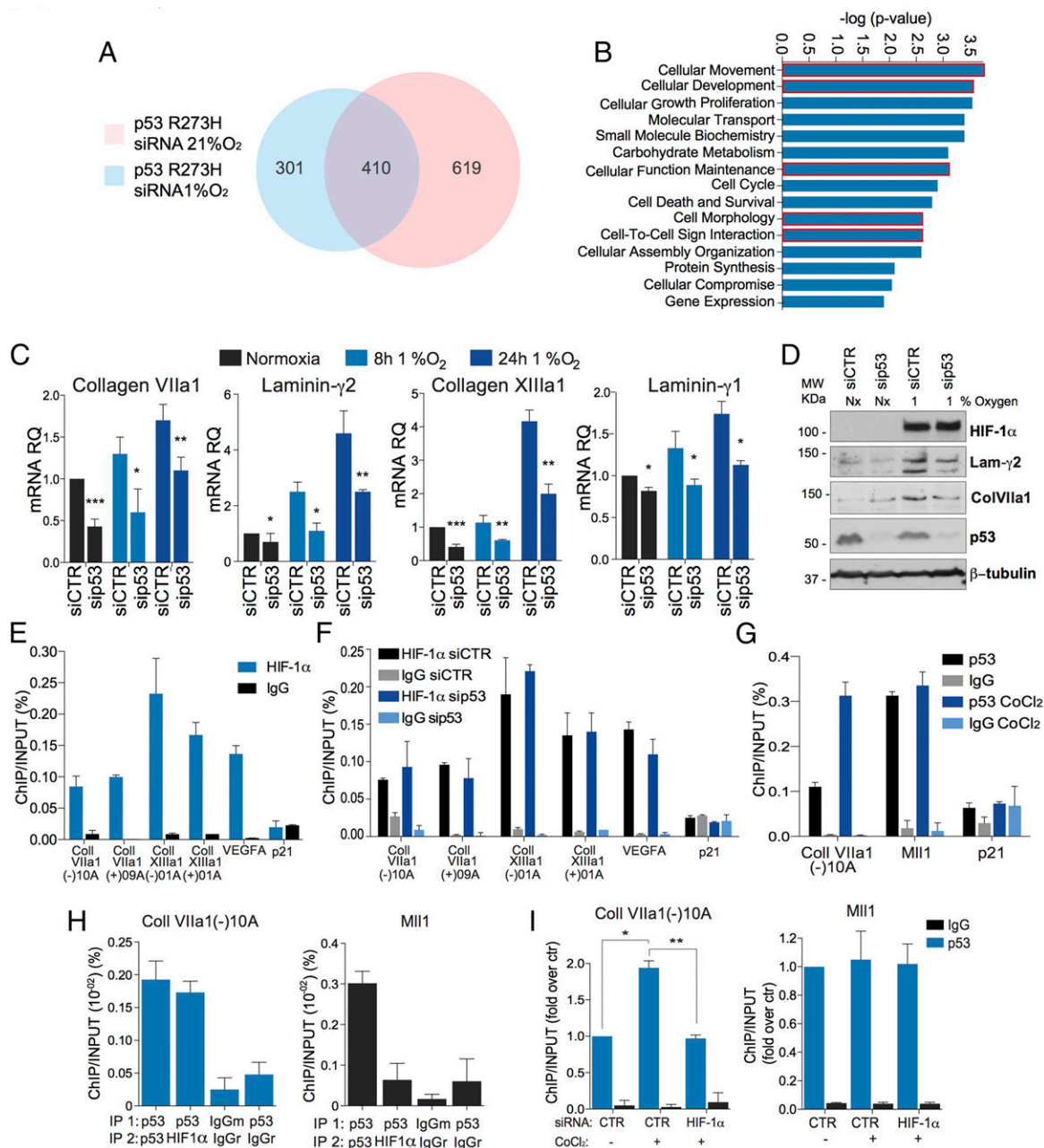
Amelio et al.

Fig. 2. p53 mutants cooperate with HIF-1 in transcriptional regulation of ECM components. (*A*) Venn diagram of gene expression profiling analysis representing the distribution of genes differentially regulated by p53 R273H in NCI-H1155 cells treated with normoxia or 1% oxygen (8 h). (*B*) Pathway clustering analysis of 301 genes differentially regulated by p53 R273H in NCI-H1155 cells treated with 1% oxygen. Pathways of major interest are highlighted in red. (*C*) RT-qPCR analysis of genes encoding ECM components differentially regulated by the p53 mutants and hypoxia in NCI-H1155 cells. CTR, control. *$P < 0.05$, **$P < 0.01$, ***$P < 0.001$; paired two-tailed t test. Error bars indicate SD of independent biological replicates ($n = 3$). (*D*) Western blot analysis of Lam-γ2 and type VII collagen in whole-cell extracts of NCI-H1155 cells following knockdown of p53 R273H and exposure to 1% oxygen for 24 h. MW, molecular weight (molecular mass); Nx, normoxia. (*E*) ChIP-qPCR analysis of CoCl$_2$-treated NCI-H1155 cells for the binding of HIF-1α to response elements in the proximity of the collagen VIIa1 and collagen XIIIa1 genomic loci. (*F*) ChIP-qPCR analysis of CoCl$_2$-treated NCI-H1155 cells following mutant p53 silencing by siRNA for the binding of HIF-1α to response elements in the proximity of the collagen VIIa1 and collagen XIIIa1 genomic loci. The response element in the VEGFA and p21 genomic loci represent the positive and negative controls, respectively, for HIF-1α binding. (*G*) ChIP-qPCR analysis of CoCl$_2$-treated or untreated NCI-H1155 cells for the binding of p53 R273H to response elements in the proximity of the collagen VIIa1 genomic locus. CoCl$_2$-treated NCI-H1155 has been subjected to 4 h with 250 μM CoCl$_2$ and then collected and processed, along with the untreated cells, for ChIP assay. The Mll1 transcription starting site (TSS)-proximal peak and the p21 promoter region represent HIF-1–independent positive and negative controls for p53 mutant binding, respectively. Error bars indicate the SD of technical replicates, and the histogram shows representative ChIP-qPCR assays of four (or more) independent biological replicates. (*H*) ChIP/re-ChIP analysis for the binding of p53 R273H to a response element in the proximity of the collagen VIIa1 genomic locus performed on NCI-H1155 cells treated with 250 μM CoCl$_2$ and subjected to two subsequent immunoprecipitations (IP; as indicated in the panel). The Mll1 TSS-proximal peak represents a HIF-1–independent positive control for p53 mutant binding. Error bars indicate the SE of three biological replicates. (*I*) ChIP-qPCR assay for the binding of p53 R273H to response element in the proximity of the collagen VIIa1 genomic locus in NCI-H1155 cells following HIF-1α silencing of cells and CoCl$_2$ treatment. NCI-H1155 cells have been transfected with siRNA control or HIF-1α for 48 h. CoCl$_2$-treated NCI-H1155 cells have been treated in the last 4 h of transfection with 250 μM CoCl$_2$ and then, along with untreated cells, collected, processed, and subjected to immunoprecipitation with p53 DO-I antibody. The Mll1 TSS-proximal pick represents a HIF-1–independent positive control for p53 mutant binding. Error bars indicate the SE of three biological replicates. *$P < 0.05$, paired two-tailed t test.

analyzed the expression level in NCI-H1155 of these ECM genes, including type VIIa1 collagen (*COL7A1*), laminin-γ2 (*LAMC2*), type XIIIa1 collagen (*COL13A1*), and laminin-γ1 (*LAMC1*). RT-qPCR and Western blot analysis confirmed the ability of p53 R273H to alter the expression of these hypoxic-responsive genes (Fig. 2 *C* and *D* and *SI Appendix*, Fig. S5*D*). In addition, measurement of the levels of laminin-γ2 and type VIIa1 collagen in the culture media from hypoxic NCI-H1155 cells indicated that mutant p53 is necessary for hypoxia-mediated up-regulation and secretion of these ECM components (*SI Appendix*, Fig. S5*E*). Hypoxia-mediated up-regulation of these genes also required expression of HIF-1 (*SI Appendix*, Fig. S6*A*). Notably, type VIIa1 collagen is a critical player in epithelial tumorigenesis. The noncollagenous (NC1) domain of collagen VII strictly correlates with the tumorigenic potential of H-RAS^{V12}–transformed keratinocytes in immunodeficient mice (30). The NC1 domain of collagen VII is a ligand for laminin-332, of which laminin-γ2 is one subunit, and antibodies inhibiting laminin-332/collagen VII interaction affect tumorigenesis (31, 32). Thus, we decided to focus on type VIIa1 collagen and laminin-γ2 and expanded the analysis to additional lung cancer cell lines (NCI-H23 expressing p53 R246I and NCI-H1048 expressing p53 R273C) to confirm p53 mutant regulation of their mRNAs (*SI Appendix*, Fig. S5*F*). Laminin-γ2 appeared not to be expressed in NCI-H1048 (cycle threshold higher than 35 in RT-qPCR).

We next investigated whether mutant p53 and HIF-1 colocalize in proximal regulatory regions of the genomic loci of these genes of interest. We used the DECODE platform, which integrates text mining applications and data from the UCSC Genome Browser to compile lists of binding sites of human transcription factors. We identified two potential binding sites of HIF-1 in the proximity of the *COL7A1* genomic locus (*SI Appendix*, Fig. S6*E*). Quantitative chromatin immunoprecipitation (ChIP)-qPCR analysis confirmed the binding of HIF-1α to both regulatory regions (Fig. 2*E*), and mutant p53 expression was not required for HIF-1α binding (Fig. 2*F*). To verify that the p53 mutants occupy the same regulatory regions in a HIF-1–dependent manner, we assessed the binding of mutant p53 under basal and CoCl$_2$ conditions. ChIP-qPCR analysis revealed a significant increase in mutant p53 binding at both COL7A1 binding sites upon HIF-1 activation (Fig. 2*G* and *SI Appendix*, Fig. S7*A*). Co-occupancy of p53 R273H and HIF-1α at the *COL7A1* genomic locus was further confirmed by a ChIP/re-ChIP experiment (Fig. 2*H* and *SI Appendix*, Fig. S7*B*), and, like the subcellular fractionation results, HIF-1α depletion abolished mutant p53 accumulation upon CoCl$_2$ treatment at this site (Fig. 2*I*). Two binding sites with an analogous pattern of binding were also identified at the *COL13A1* genomic locus (*SI Appendix*, Figs. S6*D* and S7*A*).

HIF-1/p53 Mutant Complex Regulates Gene Expression by Influencing SWI/SNF Chromatin Remodeling Complex.

To explore the mechanism by which mutant p53 influences the transcriptional machinery, we tested the hypothesis that p53 R273H promotes the activity of the chromatin remodeling complex, SWI/SNF, at HIF-1–binding sites. Mutant p53 has been previously identified at the VEGFR2 promoter region in a protein complex that included SWI/SNF (33). We observed coimmunoprecipitation of the endogenous SWI/SNF subunit (i.e., BAF155, Brg1) with p53 R273H in NCI-H1155 cells (Fig. 3*A* and *SI Appendix*, Fig. S7*C*). Interaction between SWI/SNF subunits and mutant p53 was also observed in normoxic conditions, indicating the presence of a preexisting complex (Fig. 3*A* and *SI Appendix*, Fig. S7*C*). Subcellular fractionation experiments showed that SWI/SNF subunits in hypoxic NCI-H1155 cells localized to the chromatin-bound fraction following very similar time kinetics to HIF-1α and p53 R273H (Fig. 3*B*). Consistent with p53 R273H knockdown, depletion of ATPase subunits of the SWI/SNF complex, Brahma (BRM) and BRM-related gene 1 (Brg1), attenuated hypoxic-dependent up-regulation of type VIIa1 collagen and

laminin-γ2 (Fig. 3*C*). Brg1 was indeed physically identified by ChIP analysis at the genomic loci bound by the mutant p53/HIF-1 complex (Fig. 3*D* and *SI Appendix*, Fig. S7*D*). However, SWI/SNF was not required for the binding of p53 R273H and HIF-1α to the genomic regions of type VIIa1 collagen and laminin-γ2 (Fig. 3 *E* and *F*). This suggested that the SWI/SNF chromatin remodeling complex is required for the hypoxia-mediated up-regulation of these ECM components participating in chromatin organization, but not in the recruitment of the mutant p53/HIF-1 transcriptional complex. Hence, we analyzed the chromatin architecture at the type VIIa1 collagen and laminin-γ2 promoter regions, using micrococcal nuclease (MNase) digestion followed by qPCR. MNase digestion degrades DNA that is not protected from core nucleosomes (occupancy), providing a measure of chromatin accessibility. MNase analysis indicated that a relaxed, transcriptionally permissible, open chromatin was produced by 24 h of hypoxia at the type VIIa1 collagen, laminin-γ2, and VEGFA genomic regions, although expression of mut-p53 was required to support the hypoxia-induced remodeling of the chromatin architecture at the type VIIa1 collagen and laminin-γ2 sites, but not on the promoter of VEGFA (Fig. 3*G*), whose expression is not influenced by mutant p53 (*SI Appendix*, Fig. S4*A*). H3K4me and H3K27Ac at the *COL7A1* and *COL13A1* genomic regions indicated that, in NCI-H1155 cells, ColVII (−)10A and (+)09A areas represent active transcriptional enhancers (*SI Appendix*, Figs. S7 *E* and *F* and S8 *A–D*). Consistent with the result of the MNase assay, depletion of p53 R273H abolished the hypoxia-induced nucleosomal displacement at the *COL7A1* genomic site as assessed by histone H2A.Z content (Fig. 3*H*). Overall, these data indicate that mutant p53 promotes expression of HIF-1–dependent ECM components by facilitating chromatin remodeling mediated by SWI/SNF.

HIF-1/p53 Mutant/ECM Axis Induces Aggressive Phenotype of NSCLC Cells.

We next addressed the importance of this ECM signaling to the tumor-relevant phenotype of NSCLC. Exposure for 24 h to 1% O$_2$ significantly increased cellular migration and invasion, and depletion of the p53 mutants substantially reversed this effect (Fig. 4 *A* and *B* and *SI Appendix*, Fig. S9 *A–D*). The importance of type VIIa1 collagen and laminin-γ2 as downstream effectors of p53 mutant/HIF-1 protumorigenic signaling was confirmed by their capacity to revert the loss of migration and invasion potential in mutant p53-deficient hypoxic cells (Fig. 4 *A* and *B*). The specificity of type VIIa1 collagen and laminin-γ2 in the p53 mutant/HIF-1 axis was further proven by the inability of an unrelated ECM component, laminin-α5, to revert the phenotype associated with mutant p53 depletion (Fig. 4 *A* and *B*). In addition, consistent with a paracrine role exerted by ECM components, invasion of untransfected cells was altered by conditioned media derived from hypoxic cells proficient or deficient for p53 mutants (Fig. 4*C*). In agreement with a protumorigenic role of the laminin-322/collagen VII interaction (31, 32), they produced hyperactivation of AKT signaling (pAKT T308) (Fig. 4*D*). Hence, we also asked whether this axis could enhance cell growth potential in vitro and in vivo. Overexpression of laminin-γ2 or type VIIa1 collagen increased only marginally the in vitro proliferation rate of NCI-H1155 cells (Fig. 4*E*). However, we reasoned that the biological effect of the laminin-332/collagen VII-driven ECM remodeling should be assessed by recapitulating the interaction of the cancer cells, stroma, and ECM in a real tumor microenvironment. To this end, we tested whether our axis could enhance tumor growth in mouse cancer models generated by xenotransplantation of human cancer cell lines. We inoculated NCI-H1155 cells stably overexpressing laminin-γ2 or type VIIa1 collagen into immunocompromised mice. Expression of both ECM components promoted tumor growth, but type VIIa1 collagen-overexpressing cells displayed a substantial enhancement of tumor growth (Fig. 5 *A–C* and *SI Appendix*, Fig. S9 *E* and *F*). Consistently, when we deleted p53 R273H in NCI-H1155 by a
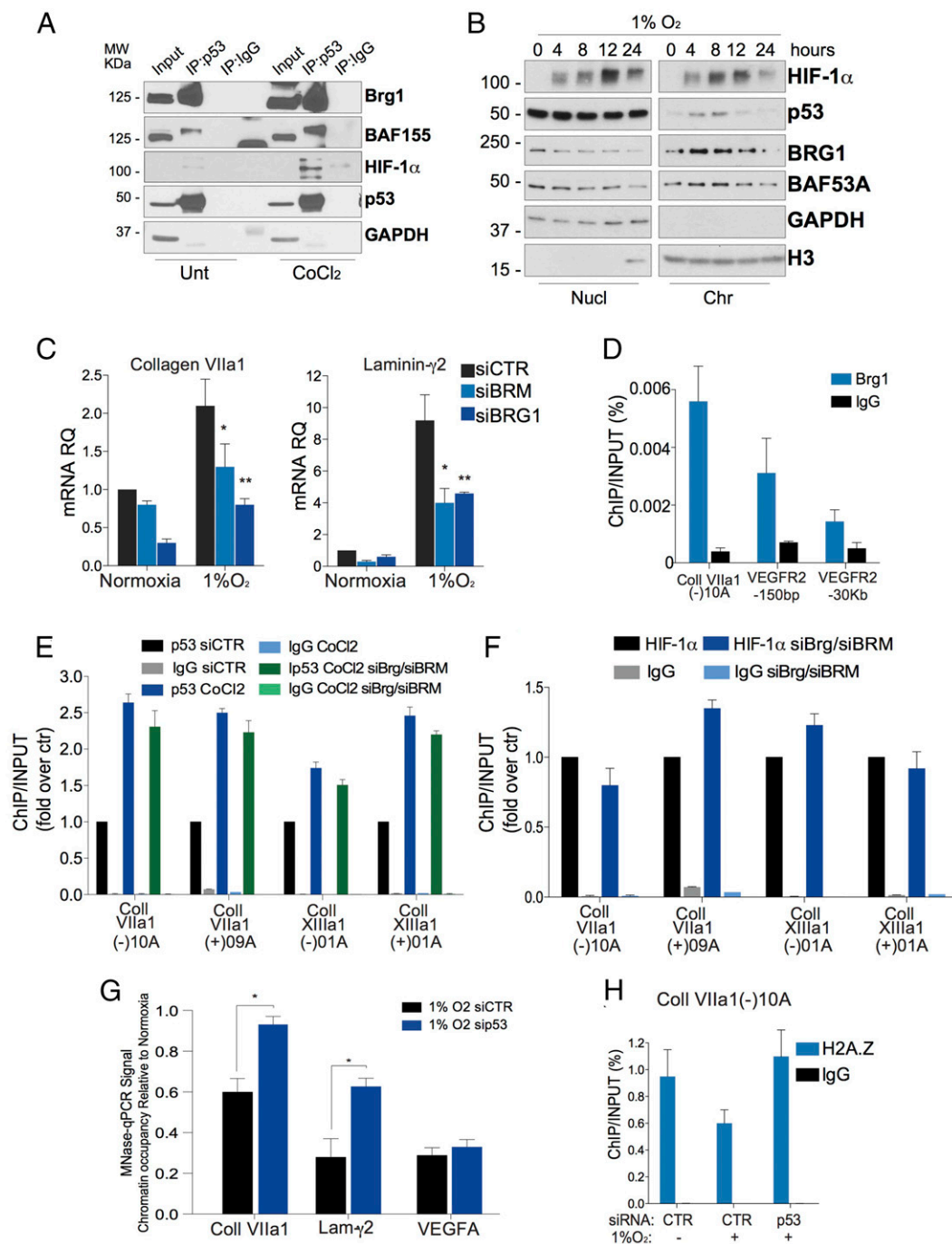
CELL BIOLOGY

Fig. 3. HIF-1/mutant p53 directly controls transcription of ECM components involving the SWI/SNF chromatin remodeling complex. (*A*) Coimmunoprecipitation assay performed by immunoprecipitating mutant p53 in untreated or CoCl$_2$-treated (for 4 h with 250 μM) NCI-H1155 cells and immunoblotting for p53, the SWI/SNF subunits (BAF155 and Brg1), HIF-1α, and the control GAPDH (4 h at 1% O$_2$). IP, immunoprecipitation; MW, molecular weight (molecular mass); Unt, untreated. (*B*) Western blot analysis of subcellular fractions (nuclear-soluble and chromatin-bound fractions) of NCI-H1155 treated with a time course (0–24 h) of 1% oxygen. Chr, chromatin-bound fraction; Nucl, soluble nuclear fraction. (*C*) RT-qPCR analysis of genes encoding ECM components following silencing of SWI/SNF ATPase subunit BRM and Brg1 in hypoxic NCI-H1155 cells (24 h at 1% O$_2$). CTR, control. *$P < 0.05$, **$P < 0.01$; paired two-tailed t test. Error bars indicate the SE of independent biological replicates ($n = 3$). (*D*) ChIP-qPCR assay for the binding of the SWI/SNF ATPase subunit Brg1 in NCI-H1155 cells treated for 4 h with 250 μM CoCl$_2$. VEGFR2 (−150 bp) and VEGFR2 (+30 Kb) represent positive and negative controls, respectively, of Brg1 binding. Error bars indicate the SE of technical replicates, and the histogram shows representative ChIP-qPCR assays of three independent biological replicates. (*E*) ChIP-qPCR analysis of CoCl$_2$-treated NCI-H1155 cells following concurrent Brg1 and BRM silencing by siRNA for the binding of mutant p53 to response elements in the proximity of the collagen VIIa1 and collagen XIIIa1 genomic loci. Error bars indicate the SE of independent biological replicates ($n = 3$). (*F*) ChIP-qPCR analysis of CoCl$_2$-treated NCI-H1155 cells following concurrent Brg1 and BRM silencing by siRNA for the binding of HIF-1α to response elements in the proximity of the collagen VIIa1 and collagen XIIIa1 genomic loci. Error bars indicate the SE of independent biological replicates ($n = 3$). (*G*) Chromatin was digested with MNase, and mononucleosome-sized DNA fragments were isolated. qPCR was performed on the promoter regions of the hypoxic-responsive genes Lam-γ2, type VII collagen, and VEGFA. Error bars represent the SE of three independent experiments. *$P < 0.05$, paired two-tailed t test. (*H*) ChIP-qPCR assay assessing the content of histone H2A.Z at the collagen VIIa1 genomic locus in p53-depleted NCI-H1155 cells following 16 h of hypoxia (at 1% O$_2$). Error bars indicate the SE of technical replicates, and the histogram shows representative ChIP-qPCR assays of three independent biological replicates.
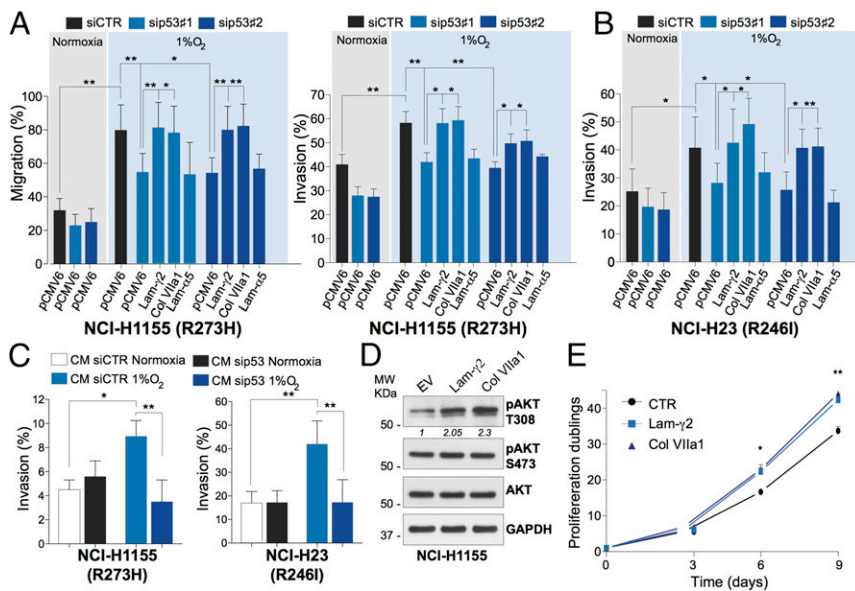
Fig. 4. Type VIIa1 collagen and laminin-γ2 promote a p53 mutant/HIF-1–dependent proinvasive phenotype. (*A* and *B*) p53 mutants affect hypoxia-mediated migration and invasion of NCI-H1155 and NCI-H23 NSCLC cells, and overexpression of type VIIa1 collagen and laminin-γ2 reverts this impairment. CTR, control; pCMV6, empty vector-transfected control cells. *$P < 0.05$, **$P < 0.02$; two-tailed paired *t* test. Error bars indicate the SE of independent biological replicates ($n = 5$ for NCI-H1155, $n = 3$ for NCI-H23). (*C*) Conditioned media (CM) from corresponding p53 mutant silenced cells treated for 24 h with 1% oxygen alter the migration and invasion capacity of NCI-H1155 and NCI-H23 NSCLC cells. *$P < 0.05$, **$P < 0.01$; two-tailed paired *t* test. Error bars indicate the SE of independent biological replicates ($n = 4$ for NCI-H1155, $n = 3$ for NCI-H23). (*D*) Western blot analysis of NCI-H1155 cells stably overexpressing type VIIa1 collagen or laminin-γ2 displays hyperactivation of pAKT T308. EV, empty vector; MW, molecular weight (molecular mass). (*E*) Proliferation doublings of NCI-H1155 cells stably overexpressing type VIIa1 collagen or laminin-γ2. *$P < 0.05$, **$P < 0.01$; paired two-tailed *t* test. Error bars indicate the SE of independent biological replicates ($n = 4$).

doxycycline-responsive inducible CRISPR/Cas9 system (*SI Appendix,* Fig. S9G), tumor growth of hypoxic preconditioned cells was dramatically reduced, and this was significantly reverted by reexpression of laminin-γ2 or type VIIa1 collagen (Fig. 5 *D–F* and *SI Appendix,* Fig. S9H). Together, our data demonstrate the ability of p53 mutants to promote a tumor-relevant phenotype through modulation of ECM components by a GOF effect on HIF-1.

ECM Signature Correlates with Hypoxia and p53 Mutants in Human NSCLC with Poor Prognosis. Next, we validated whether the synergistic effect of mutant p53 and HIF-1 on the regulation of ECM components was present in human NSCLC. First, we assessed whether mutant p53 and HIF-1 influenced the expression levels of the ECM genes of interest in patients with NSCLC. We extracted RNA from 45 surgically resected tumor tissues and performed RT-qPCR analysis to evaluate HIF-1 activation, assessed by the expression level of 10 well-established HIF-1 targets (hypoxia signature) and our genes of interest. Next, we calculated the Pearson correlation coefficients between the expression of our genes of interest and the hypoxia signature. We stratified the samples according to the p53 mutational status, and we observed that the Pearson correlation coefficient between the hypoxia signature and type VIIa1 collagen or laminin-γ2 expression was significant exclusively in the samples expressing mutant p53 ($R = 0.58$ for COL7A1 and $R = 0.70$ for Lam-γ2) (Fig. 6 *A* and *B*). We also analyzed the expression level of our genes of interest in "low-hypoxia" and "high-hypoxia" tumors following stratification for p53 mutational status. Here, expression levels of type VIIa1 collagen and laminin-γ2 were selectively increased in high-hypoxia tumors expressing a mutant form of p53 (*SI Appendix,* Fig. S10 *A* and *B*). To confirm these data at the protein level, we employed a human adenocarcinoma tissue microarray, including 275 cores of 110 clinical cases. More than 60% of the cases showed moderate to high expression of laminin-γ2 (Fig. 6C and *SI Appendix,* Fig. S10C). Analysis of the expression of a hypoxic marker, such as carbonic anhydrase IX (CAIX), and laminin-γ2 also confirmed that the correlation between hypoxia and our ECM signature is present exclusively in tumors expressing mutant p53 (Fig. 6 *C* and *D* and *SI Appendix,* Fig. S10D). Both CAIX and laminin-γ2 were associated with histological invasion patterns predominantly in mutant p53 cores (Fig. 6 *C* and *D*), thus confirming the existence of a synergism between hypoxic signaling and p53 mutations. We next analyzed larger cohorts of patients to further validate the clinical

data. To this end, we developed p53MutaGene, a computational tool designed to assess the effect of the p53 status on gene regulation (34). The algorithm stratified a cohort of ~300 patients with NSCLC according to p53 mutational status and computed the correlation between the expression of our genes of interest and the activation of HIF-1 (measured as the expression of direct HIF-1 target genes). Strikingly, p53MutaGene reported statistically significant differential coexpression of HIF-1 targets and our genes of interest between samples expressing wt p53 and those expressing mutant p53 (Fig. 6 *E* and *F* and *SI Appendix,* Fig. S11 *A* and *B*). Mutant p53 expression was always associated with a higher positive Pearson correlation coefficient. Analysis of the Molecular Taxonomy of Breast Cancer International Consortium (METABRIC) human cancer dataset also revealed a very similar trend in breast cancer (*SI Appendix,* Fig. S11 *C–E*). Our analyses confirm that p53 mutants can potentiate the ability of HIF-1 to drive the expression of ECM components in a clinical setting. In support of this, we also identified a tendency for mutual exclusivity between mutant p53 and laminin-γ2 genomic locus amplification in human NSCLC datasets (*SI Appendix,* Fig. S12C).

Finally, to validate the impact of this signaling pathway on cancer progression, we evaluated the clinical outcomes of patients highly expressing genes belonging to the mutant p53/HIF-1 signature. Survival analysis of NSCLC datasets (35), computed by grouping our samples into cohorts expressing high levels of type VIIa1 collagen and laminin-γ2, revealed that patients with elevated expression of this gene signature had a shorter lifespan (Fig. 6G and *SI Appendix,* Fig. S12 *A* and *B*). Consistently, high levels of type VIIa1 collagen and laminin-γ2 were significantly associated with more aggressive NSCLC (*SI Appendix,* Fig. S12D).

These data, based on analysis of clinical material from patients who had cancer, demonstrate the existence in a human disease setting of a molecular axis involving HIF-1/mutant p53/ECM and indicate that this signaling is preferentially associated with the most aggressive tumors.

Discussion

Our data reveal a GOF mechanism of p53 mutants on the transcriptional activity of HIF-1 in hypoxic NSCLC cells. The interplay between the wt members of the p53 family and HIFs has long been a subject of intense study, and reciprocal regulation between these two families of genes has been shown (15, 22, 36). Mutations in the *TP53* gene and activation of HIF-1 in

hypoxic areas are frequently observed in advanced cancer, including NSCLC. Our data indicate that co-occurrence of these two events is associated with a significantly worse prognosis (Fig. 1A). The results of our study shed light on the molecular determinants underlining the aggressive phenotype of these tumors. Here, we identify a direct interplay between mutant forms of p53 and HIF-1 in NSCLC cells.

We observed a physical interaction between p53 mutants and the regulatory subunit of HIF-1, HIF-1α. The result of this interaction is the formation of a transcriptional complex that regulates expression of downstream targets, such as the ECM components type VIIa1 collagen and laminin-γ2. In particular, while HIF-1α recruits and shuttles mutant p53 to the DNA genomic elements, mutant p53 does not influence HIF-1 binding to the DNA but impinges on its transcriptional activity. The binding of mutant p53 to the genomic elements is, however, not completely abolished by HIF-1α depletion, indicating that other factors also participate in this process. The cooperation of p53 mutants and HIF-1 in the transcriptional regulation of ECM genes involves chromatin remodeling mediated by the SWI/SNF complex, in keeping with a recent study by Prives and coworkers (33) that implicated SWI/SNF activity in the p53 mutant-dependent transcriptional regulation of VEGF-R2 in breast cancer cells. Mechanistically, the SWI/SNF complex does not influence the binding of mutant p53/HIF-1 to the genomic sites of the ECM genes. However, its ATPase subunits Brg1 and BRM are required for the hypoxia-induced up-regulation of type VIIa1 collagen and laminin-γ2, probably by mediating the mutant p53-dependent changes in the chromatin architecture. The impact of p53 mutants on the cancer cell epigenome and chromatin organization therefore appears to be a potential key mechanistic aspect for p53 mutants oncogenic properties and consequentially also an important therapeutic avenue to explore.

Type VIIa1 collagen and laminin-γ2 critically contribute to the HIF-1/mutant p53-dependent tumor phenotype. Our in vivo and in vitro studies demonstrated that reexpression of laminin-γ2 and type VIIa1 collagen in NSCLC cells reverts the tumorigenic properties lost upon depletion of the endogenous mutant p53. Importantly, correlation of the expression of these ECM genes with HIF-1 activation is observed only in human NSCLC carrying p53 mutations, and this observation was consistently reproduced in different settings: mRNA of a cohort of 45 surgically resected NSCLCs; tissue microarray of ~100 NSCLCs; and large, publicly available gene expression profile datasets of lung cancers. Remarkably, laminin-γ2 in hypoxic p53 mutant human NSCLC is associated with an invasive histological pattern that represents a hallmark of advanced tumor areas.

A major implication of our findings is indeed the flexibility of p53 mutants in acquiring selective GOF properties under specific cellular stress conditions. Our data clearly imply that in hypoxic tumors, p53 mutants can acquire protumorigenic properties not observed under other conditions. This flexibility can be expanded also to intratumoral heterogeneity and plasticity, which can give rise to specific tumor areas where the synergistic activity of
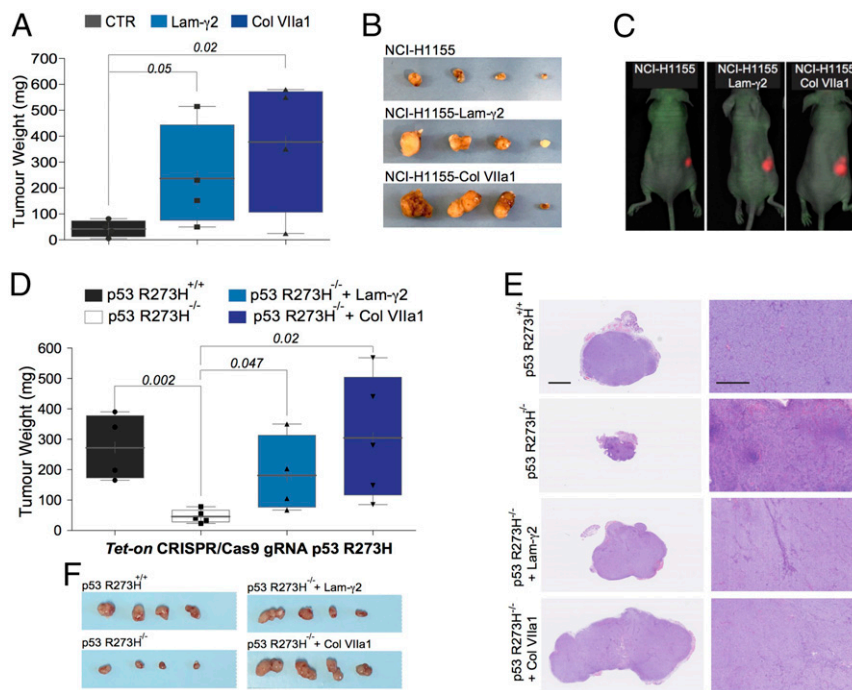

Fig. 5. Type VIIa1 collagen and laminin-γ2 promote the p53 mutant/HIF-1–dependent protumorigenic phenotype in vivo. (A and B) NCI-H1155 cells stably overexpressing type VIIa1 collagen or laminin-γ2 injected s.c. into immunocompromised mice grow faster than empty vector-transfected cells. (A) Columns indicate distribution of tumor weight. Gray lines indicate the average of the distribution. P values are indicated in the corresponding panel (unpaired two-tailed t test; n = 4 for NCI-H1155 cells, NCI-H1155 CollVIIa1 and Lam-γ2). CTR, control. (B) Photographs of tumors after dissection. Full photography of tumors after dissection is shown in SI Appendix, Fig. S9E. (C) Composite images of mice and fluorescent tumor signals (mCherry) were acquired a day before the end point using an IVIS Spectrum In Vivo Imaging System (PerkinElmer). (D–F) Genetic deletion of p53 R273H by inducible CRISPR/Cas9 in NCI-H1155 cells significantly impairs tumor growth after s.c. transplantation in immunocompromised mice, and overexpression of type VIIa1 collagen or laminin-γ2 reverts this effect. NCI-H1155 Tet-On guide RNA (gRNA) p53 cells (parental, type VIIa1 collagen-overexpressing, or laminin-γ2–overexpressing) were treated for 72 h with 2 µg/mL doxycycline and exposed for the last 24 h before injection with 1% oxygen. (D) Columns indicate distribution of tumor weight. Gray lines indicate average of the distribution. P values are indicated in the corresponding panel (two-tailed unpaired t test; n = 4 for p53 R273H+/+ and p53 R273H−/− laminin-γ2 groups, n = 5 for p53 R273H−/− and p53 R273H−/− type VII collagen groups). (E) Representative hematoxylin/eosin images of xenograft tumors from F. (Scale bars: Left, 2 mm; Right, 500 µm.) (F) Photographs of tumors after dissection. Full photography of tumors after dissection is shown in SI Appendix, Fig. S9H.
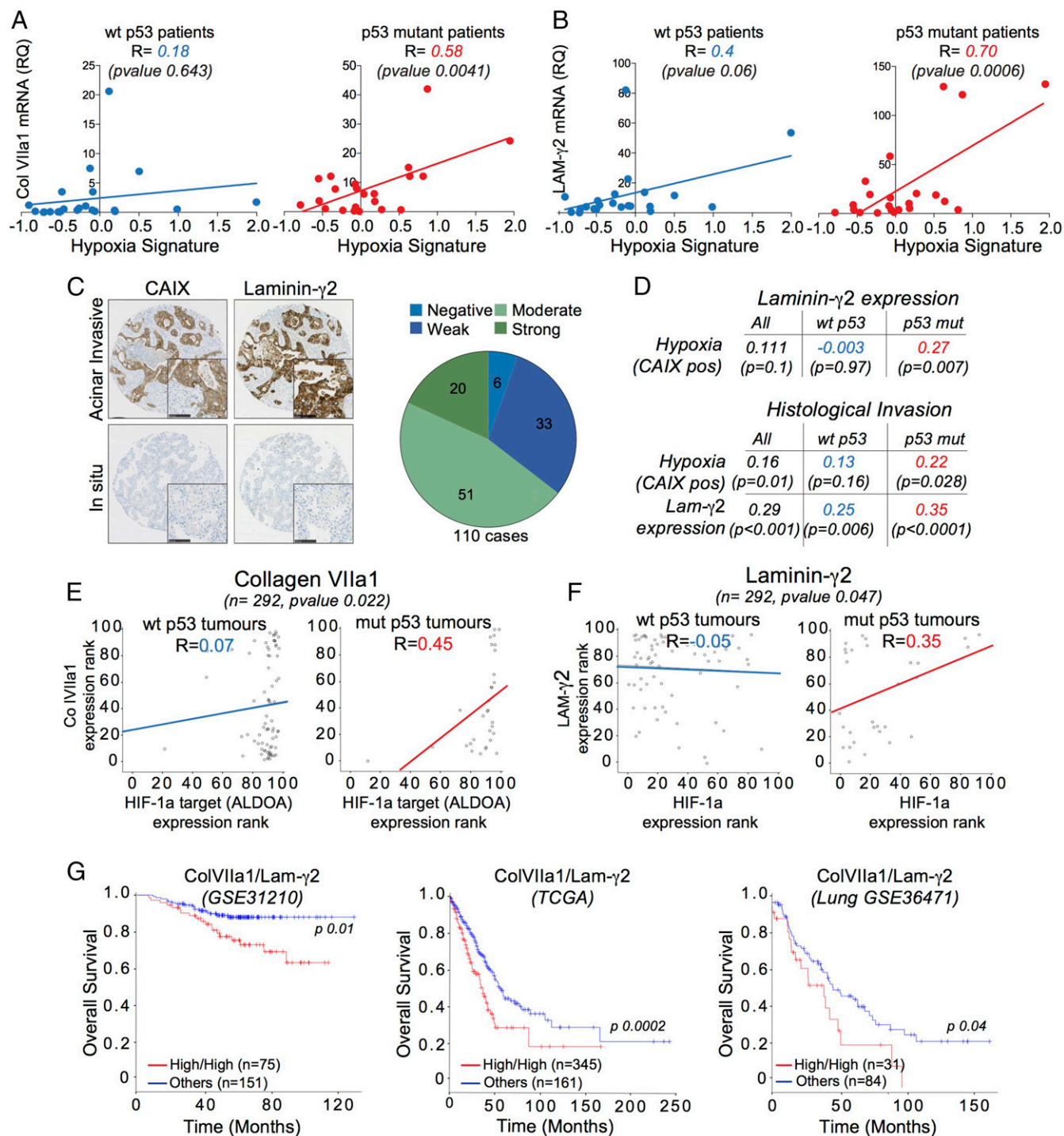
Fig. 6. p53 mutants and HIF-1 synergistically act in human NSCLC. (A and B) Correlation analysis of mRNA expression levels in surgically resected human NSCLC specimens based on RT-qPCR in blue samples expressing wt p53 and in red samples expressing mutant p53. P values are indicated in the corresponding panel (wt p53, $n = 22$; p53 mutant, $n = 23$). R, Pearson correlation coefficient; RQ, relative quantification. (C, Left) Representative images of the immunohistochemical staining for CAIX and Lam-γ2 on the human lung adenocarcinoma tissue microarray. (C, Right) Pie chart reports the median distribution of Lam-γ2 staining in the 110 cases analyzed. (Scale bar: 100 μm.) (D) Correlation between expression of CAIX and Lam-γ2 (Upper) and the correlation between histological invasion and CAIX or Lam-γ2 (Lower) are shown. Correlation coefficients have been calculated as Spearman's rho. P values are indicated in the corresponding panel. Computation has been performed on tumor cores (All, $n = 210$; p53 wt, $n = 111$; p53 mut, $n = 99$). pos, positive. (E and F) Correlations between the expression of HIF-1 targets and our genes of interest, Col VIIa1 and Lam-γ2, were computed in two cohorts of a human NSCLC dataset (GSE36471) stratified according to p53 status ($n = 292$; Pearson correlation coefficients and P values are indicated in the corresponding panel). ALDOA, Aldolase A. (G) Kaplan–Meier plots indicating the overall survival estimates for patients with NSCLC expressing high levels of Col VIIa1 and Lam-γ2. P values are indicated in the corresponding panel. TCGA, The Cancer Genome Atlas.

hypoxic-driven HIF-1 and p53 mutations produces tissue niches with a high degree of aggressiveness that favors evolution of the tumor to a lethal phenotype.

Our results shed light on the molecular determinants potentially implicated in advanced stages of tumorigenesis. In addition, these findings highlight potential novel therapeutic interventions aimed

Amelio et al.

at targeting the mutant p53/HIF-1 interaction to minimize the dissemination of human NSCLC.

Materials and Methods

Xenotransplanted Tumor Model. BALB/c nude l (nu/nu) mice were purchased from Charles River Laboratories and then housed in the central research facility of the University of Leicester. All experimental work involving animals was approved by the local ethical committee and performed in accordance with United Kingdom legislation. The experiment was performed on sex-matched, age-matched, and strain-matched mice. All of the experiments have been performed by s.c. injection into 6- to 8-wk-old nu/nu mouse 1×10^6 NCI-H1155 cells resuspended in DMEM/F12 (1:1) medium (Invitrogen). Two weeks after injection, tumors were collected, weighed using an Analytical Balance Scale (Fischer Brand), fixed in 4% paraformaldehyde (48 h), and embedded in paraffin. For the experiment with prior injection of tetracycline (Tet)-On–inducible NCI-H1155 cells, cells were treated for 72 h with doxycycline (2 μg/mL) and 24 h of 1% oxygen exposure. Hematoxylin/eosin staining was performed as previously described (37) on paraffin-embedded sections. In brief, after deparaffinization and rehydration, the sections were stained for 5 min with hematoxylin, and then washed in distilled water for 3 min and incubated for 1 min in 1% HCl/70% alcohol. The sections were then washed in distilled water and stained for 1 min in 1% eosin. The images were captured with a Hamamatsu NanoZoomer XR digital pathology slide scanner, and images were processed with NDP. view.2.3.1 software (Hamamatsu).

Generation of Tet-On–Inducible NCI-H1155 CRISPR/Cas9 Cells. For generation of an inducible CRISPR/Ca9 system, we employed the previously described system based on FUCas9Cherry and FgH1UTG plasmids (38). NCI-H1155 cells were infected with lentiviral vectors carrying expression of constitutive Cas9 (FUCas9Cherry) and doxycycline-inducible guide RNA (FgH1UTG). To produce lentiviral particles, 293T cells were transiently transfected with vector DNA, along with the packaging constructs pMDLg/pRRE (catalog no. 12251; Addgene), pRSV-rev (catalog no. 12253; Addgene), and pMD2.G (catalog no. 12259; Addgene), and the target plasmid using Effectene transfection reagent (catalog no. 301425; Qiagen) according to the guidelines provided. Virus-containing supernatants were collected at 48 h after transfection and filtered with a 0.45-μm filter. NCI-H1155 cells were infected with a suspension of virus-containing supernatant with 8 μg/mL polybrene and incubated for 24 h at 37 °C. Virally transduced cell lines were then sorted using a FACSAriaII (Becton Dickinson) flow cytometer. All cells positive for mCherry (FUCas9Cherry) and EGFP (FgH1UTG) were sorted to produce a whole population of double-positive cells. To induce single-guide RNA (sgRNA) expression, virally transduced and sorted cells were treated for 72 h with 2 μg/mL doxycycline hyclate (D9891; Sigma). The Massachusetts Institute of Technology CRISPR design software was used for the design of sgRNAs (crispr.mit.edu). Detailed material and methods are provided in *SI Appendix, Supplementary Materials and Methods*.

1. Freed-Pastor WA, Prives C (2012) Mutant p53: One name, many proteins. *Genes Dev* 26:1268–1286.
2. Vousden KH, Prives C (2009) Blinded by the light: The growing complexity of p53. *Cell* 137:413–431.
3. Freed-Pastor WA, et al. (2012) Mutant p53 disrupts mammary tissue architecture via the mevalonate pathway. *Cell* 148:244–258.
4. Zhu J, et al. (2015) Gain-of-function p53 mutants co-opt chromatin pathways to drive cancer growth. *Nature* 525:206–211.
5. Weissmueller S, et al. (2014) Mutant p53 drives pancreatic cancer metastasis through cell-autonomous PDGF receptor β signaling. *Cell* 157:382–394.
6. Kastenhuber ER, Lowe SW (2017) Putting p53 in context. *Cell* 170:1062–1078.
7. Kim MP, Lozano G (2018) Mutant p53 partners in crime. *Cell Death Differ* 25:161–168.
8. Pfister NT, Prives C (2017) Transcriptional regulation by wild-type and cancer-related mutant forms of p53. *Cold Spring Harb Perspect Med* 7:a026054.
9. Do PM, et al. (2012) Mutant p53 cooperates with ETS2 to promote etoposide resistance. *Genes Dev* 26:830–845.
10. Bieging KT, Attardi LD (2015) Cancer: A piece of the p53 puzzle. *Nature* 520:37–38.
11. Bieging KT, Mello SS, Attardi LD (2014) Unravelling mechanisms of p53-mediated tumour suppression. *Nat Rev Cancer* 14:359–370.
12. Semenza GL (2012) Hypoxia-inducible factors: Mediators of cancer progression and targets for cancer therapy. *Trends Pharmacol Sci* 33:207–214.
13. Keith B, Johnson RS, Simon MC (2011) HIF1α and HIF2α: Sibling rivalry in hypoxic tumour growth and progression. *Nat Rev Cancer* 12:9–22.
14. Semenza GL (2012) Hypoxia-inducible factors in physiology and medicine. *Cell* 148:399–408.
15. Amelio I, Melino G (2015) The p53 family and the hypoxia-inducible factors (HIFs): Determinants of cancer progression. *Trends Biochem Sci* 40:425–434.
16. Rankin EB, Giaccia AJ (2016) Hypoxic control of metastasis. *Science* 352:175–180.
17. Gilkes DM, Semenza GL, Wirtz D (2014) Hypoxia and the extracellular matrix: Drivers of tumour metastasis. *Nat Rev Cancer* 14:430–439.
18. Ivan M, et al. (2001) HIFalpha targeted for VHL-mediated destruction by proline hydroxylation: Implications for O2 sensing. *Science* 292:464–468.
19. An WG, et al. (1998) Stabilization of wild-type p53 by hypoxia-inducible factor 1alpha. *Nature* 392:405–408.
20. Graeber TG, et al. (1994) Hypoxia induces accumulation of p53 protein, but activation of a G1-phase checkpoint by low-oxygen conditions is independent of p53 status. *Mol Cell Biol* 14:6264–6277.
21. Blagosklonny MV, et al. (1998) p53 inhibits hypoxia-inducible factor-stimulated transcription. *J Biol Chem* 273:11995–11998.
22. Ravi R, et al. (2000) Regulation of tumor angiogenesis by p53-induced degradation of hypoxia-inducible factor 1alpha. *Genes Dev* 14:34–44.
23. Kaluzová M, Kaluz S, Lerman MI, Stanbridge EJ (2004) DNA damage is a prerequisite for p53-mediated proteasomal degradation of HIF-1alpha in hypoxic cells and downregulation of the hypoxia marker carbonic anhydrase IX. *Mol Cell Biol* 24:5757–5766.
24. Leszczynska KB, et al. (2015) Hypoxia-induced p53 modulates both apoptosis and radiosensitivity via AKT. *J Clin Invest* 125:2385–2398.
25. Olcina MM, et al. (2016) H3K9me3 facilitates hypoxia-induced p53-dependent apoptosis through repression of APAK. *Oncogene* 35:793–799.
26. Hammond EM, et al. (2006) Genome-wide analysis of p53 under hypoxic conditions. *Mol Cell Biol* 26:3492–3504.
27. Xiong S, et al. (2014) Pla2g16 phospholipase mediates gain-of-function activities of mutant p53. *Proc Natl Acad Sci USA* 111:11145–11150.
28. Oldham WM, Clish CB, Yang Y, Loscalzo J (2015) Hypoxia-mediated increases in L-2-hydroxyglutarate coordinate the metabolic response to reductive stress. *Cell Metab* 22:291–303.
29. Intlekofer AM, et al. (2015) Hypoxia induces production of L-2-hydroxyglutarate. *Cell Metab* 22:304–311.
30. Ortiz-Urda S, et al. (2005) Type VII collagen is required for Ras-driven human epidermal tumorigenesis. *Science* 307:1773–1776.
31. Waterman EA, et al. (2007) A laminin-collagen complex drives human epidermal carcinogenesis through phosphoinositol-3-kinase activation. *Cancer Res* 67:4264–4270.
32. Marinkovich MP (2007) Tumour microenvironment: Laminin 332 in squamous-cell carcinoma. *Nat Rev Cancer* 7:370–380.
33. Pfister NT, et al. (2015) Mutant p53 cooperates with the SWI/SNF chromatin remodeling complex to regulate VEGFR2 in breast cancer cells. *Genes Dev* 29:1298–1315.
34. Amelio I, Knight RA, Lisitsa A, Melino G, Antonov AV (2016) p53MutaGene: An online tool to estimate the effect of p53 mutational status on gene regulation in cancer. *Cell Death Dis* 7:e2148.
35. Amelio I, et al. (2016) SynTarget: An online tool to test the synergetic effect of genes on survival outcome in cancer. *Cell Death Differ* 23:912.
36. Amelio I, et al. (2015) TAp73 opposes tumor angiogenesis by promoting hypoxia-inducible factor 1α degradation. *Proc Natl Acad Sci USA* 112:226–231.
37. Amelio I, et al. (2012) miR-24 triggers epidermal differentiation by controlling actin adhesion and cell migration. *J Cell Biol* 199:347–363.
38. Aubrey BJ, et al. (2015) An inducible lentiviral guide RNA platform enables the identification of tumor-essential genes and tumor-promoting mutations in vivo. *Cell Rep* 10:1422–1432.